Chapter 8

Impact of 13-93 bioactive glass addition on the tribological behavior of 3Y-TZP-based biocomposite materials

8.1 Introduction

3Y-TZP-based bioactive glass (BG) biocomposite materials hold significant potential for use as restorative materials in dentistry (Ho *et al.*, 2011) (de Paula *et al.*, 2019) (Habibe *et al.*, 2009). Therefore, it is essential to evaluate not only their mechanical and biological properties but also their tribological behavior. Dental restorative materials are subjected to sliding contact and various loads during chewing, where friction and wear are influenced by factors such as surrounding parameters (including pH, oxygen levels, and abrasiveness), the type of applied load, and the inherent properties of the materials (Pandey *et al.*, 2014) (Buciumeanu *et al.*, 2018). Many researchers have studied the coefficient of friction, wear rate, and wear mechanism of zirconia and also modified zirconia (Pandey *et al.*, 2014) (Buciumeanu *et al.*, 2018). The results suggest that there is an improvement in COF and wear rate after hydrothermal treatment (Pandey *et al.*, 2014). The addition of bioactive compounds does not affect the tribological performance. Wear rates and coefficient of friction remain unchanged (Buciumeanu *et al.*, 2018). The viability of creating surface micro textures improves 3Y-TZP ceramics' wettability and tribological characteristics (Buciumeanu *et al.*, 2018). Research on the wear resistance of tooth and restorative materials has been conducted in electrolytes like distilled water, synthetic saliva, or acidic substances such as citric acid. However, for biomedical implant applications, it is recommended to conduct tribological and electrochemical testing in simulated body fluid (SBF) (Injeti *et al.*, 2019).

The objective of this work is to synthesize the 3Y-TZP/13-93BG bioceramic composites. Sample identification and different compositions of biocomposite materials are given in Table 3.1. This chapter investigates the effect of bioactive glass addition on the tribological behavior of composite materials [(100-x) (3Y-TZP) – x (13-93 BG)] where x = 0 to 25 wt%] in simulated body fluid (SBF).

8.2 Results and discussion

8.2.1 Coefficient of friction (COF) study

Fig. 8.1 represents the Image of prepared sintered composite samples which are used for the tribological behavior study. For all prepared composites, the coefficient of friction (COF) changes with the number of cycles and variation of bioactive glass (BG) concentration, as represented in Fig. 8.2(a) & Fig. 8.2(b) respectively. Fig. 8.2(a) shows the COF vs. running cycle of 3Y-TZP and 3Y-TZP -BG composite at 20 N load. Results indicate that the COF value for all samples initially increases up to 200 cycles. After that, it decreases up to 400 cycles. Between 400 to 1000 cycles, all samples follow a decreasing and increasing trend. After 1000 cycles, all samples become steady and follow the almost constant trend. The observed pattern may be probably attributed to the early cycles, during which the tribo-pairs display a greater degree of strong asperity contacts. As the cycle progresses, these acute asperities wear and break, resulting in a smoother surface and lower COF values (Pandey *et al.*, 2023). An additional reason could be that the worn debris between the mating parts works as a lubricant mixed with the SBF solution, lowering the COF (Kumar *et al.*, 2024).

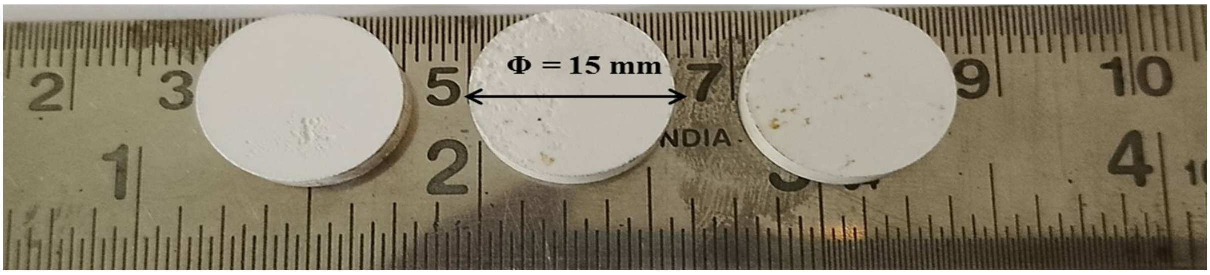

Fig. 8.1 Image of prepared sintered composite samples.

Fig. 8.2(b) shows the graph between the COF and composite samples. Results show that the average COF value of the ZBG0 sample attains a maximum value (0.26) shortly after the experiment, and then further decreases up to the ZBG10 sample. The minimum value of average COF (0.17) is found for the ZBG10 samples. After that, the value of average COF increases with BG content up to the ZBG25 sample. Incorporating BG up to 10 wt% into 3Y-TZP ceramics improves mechanical properties, such as hardness and flexural strength as reported previously in Table 4.2 of Chapter 4, which can influence wear resistance and coefficient of friction. Porosity is also an important parameter that affects the COF (Pandey *et al.*, 2023) (Kumar *et al.*, 2024).

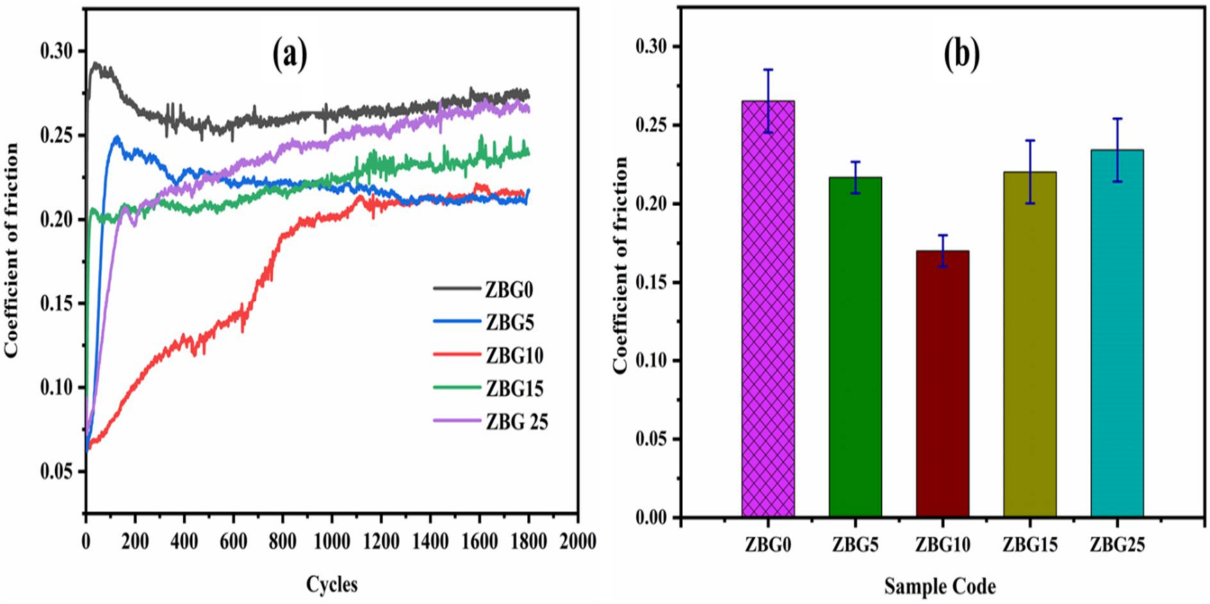

Fig. 8.2 (a) Coefficient of friction vs running cycles, (b) Coefficient of friction vs bioactive glass concentration. The average friction coefficient of sintered composite samples running after 1800 cycles at 20 N load.

The porosity is highest in the ZBG0 sample and lowest in the ZBG10 sample, as reported in Table 4.1 of Chapter 4. The microstructure of the composite samples may also affect the COF. As previously stated the microstructure of the ZBG10 sample is compacted due to the mixing of BG particles into the 3Y-TZP, the crystalline grains of 3Y-TZP are partially wetted with BG frits at 1250ºC and compacted with each other, resulting in improved mechanical properties of the 3Y-TZP as discussed in Chapter 4. The compact arrangement caused by minimal open porosity enhances the cohesion among particles, improving both performance and surface smoothness. This, in turn, minimizes the coefficient of friction (COF) of the ZBG10 sample to its lowest level (Huang *et al.*, 2019). Furthermore, porosity increases with the addition of BG concentrations above 10 wt% Table 4.1 of Chapter 4. This increased porosity disrupts the surface smoothness of the ZBG15 and ZBG25 samples, resulting in a higher COF. Overall, incorporating BG into 3Y-TZP ceramics can potentially reduce the COF with up to 10 wt% BG addition, but further addition of up to 25 wt% increases the COF.

8.2.2. Width, depth, and area of wear scar

The wear scar profiles of all composite samples, obtained by the profilometer are shown in Fig. 8.3. The width, depth, and area of the wear scar of the 2D profile are quantified, calculated, and tabulated in Table 8.1.

Table 8.1 The cross-sectional area of wear scar, width of wear scar, average wear depth, wear volume, and wear rate of composite samples.

Samples	Cross-sectional area of wear scar A_w (μm^2)	Width of wear scar W_w (μm)	Depth of wear scar W_d (μm)	Wear volume (mm^3)	Wear rate (mm^3/mm of sliding distance) ×10^{-5}
ZBG0	715364.65	3595.9	198.93	4.1901	23.28
ZBG5	270290.03	2701.3	100.05	1.5076	8.38
ZBG10	21725.56	1173.5	18.51	0.1140	0.63
ZBG15	406326.34	3234.6	125.61	2.2774	12.65
ZBG25	496185.03	3344.2	148.37	2.8232	15.68

As shown in Table 8.1, the depth of wear scar of the ZBG10 sample is the lowest (18.51 µm) among all the composite samples, while the maximum depth (198.93 µm) is observed for the ZBG0 sample. Table 8.1, also shows the cross-sectional area (A_w) and width (W_w) of the wear scar of composite samples are significantly depend on the BG concentration (0, 5, 10, 15, and 25 wt%). Both A_w and W_w first decrease up to 10 wt% of BG and afterward start to increase up to 25 wt% of BG. The maximum value of A_w (715364.65 µm^2) and W_w (3595.9 µm) is found for the ZBG0 sample and the minimum value of A_w (21725.56 µm^2) and W_w (1173.5 µm) for the ZBG10. According to reports, the depth and width of the wear scar primarily depend on the material's hardness, density, microstructure, and elastic modulus (Pandey *et al.*, 2023) (Kumar *et al.*, 2024) (Fellah *et al.*, 2013). The depth of material wear is contingent upon the hardness of the opposing material (Pandey *et al.*, 2023) (Kumar *et al.*, 2024) (Fellah *et al.*, 2013) (Iijima *et al.*, 2003). As stated in Chapter 4, the density and mechanical properties of the ZBG10 sample are the highest compared to the other sample. Simultaneously, Vickers micro-hardness is also good for the ZBG10 sample. So these properties of the developed composite (ZBG10) enhance the wear resistance of the samples and reduce the wear scar area.

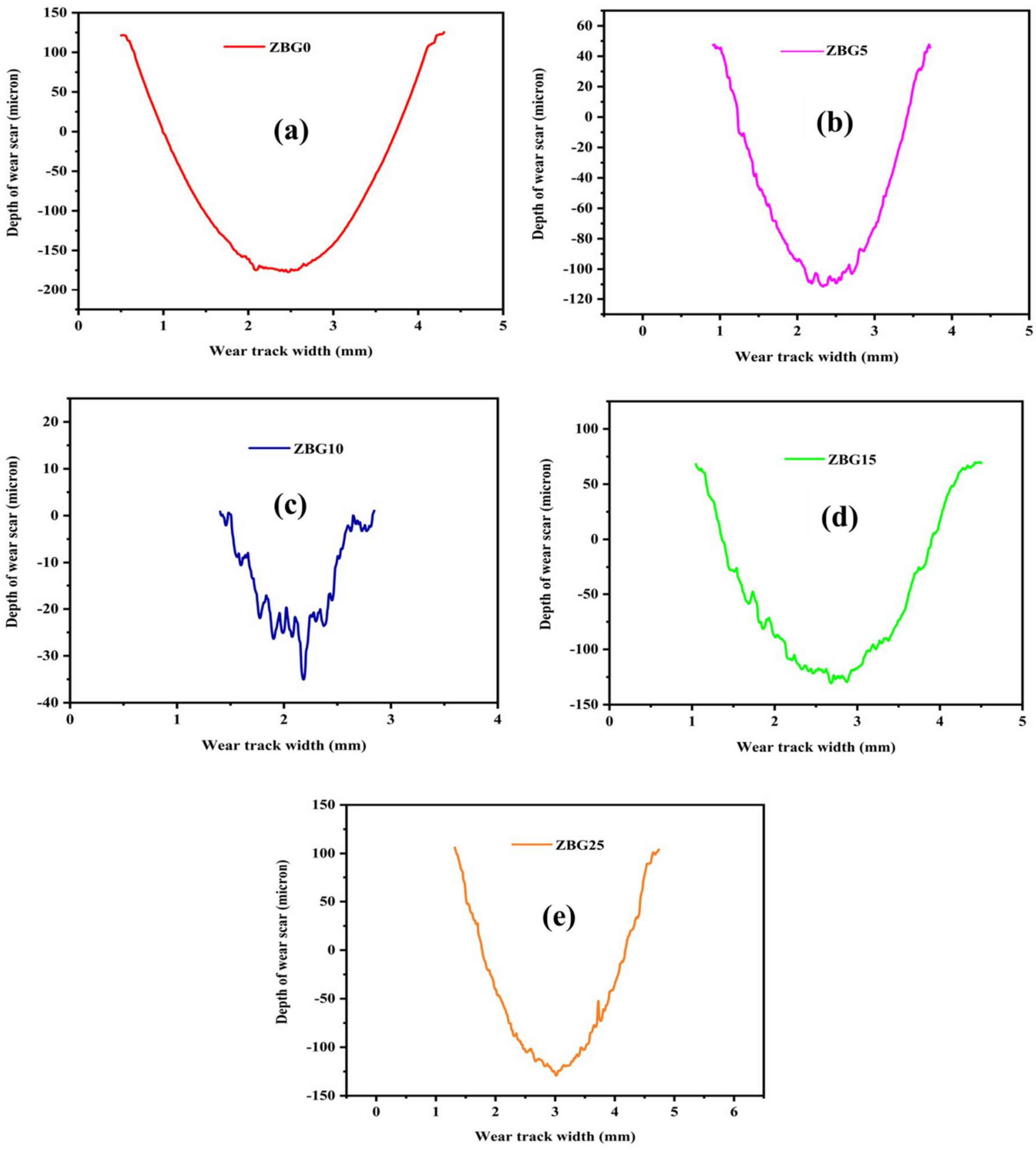

Fig. 8.3 Wear scar profile of all sintered composite samples obtained from profilometer.

8.2.3 Wear volume and wear rate

Table 8.1 demonstrates how the wear rate varies with BG concentration (0, 5, 10, 15, and 25 wt%). Notably, the ZBG0 sample exhibits the highest wear rate at 23.28 × 10^{-5} (mm^3/mm), whereas the ZBG10 sample displays the lowest wear rate at 0.63 × 10^{-5} (mm^3/mm). Additionally, the wear rate increases with higher BG concentrations for samples

ZBG15 and ZBG25. Based on these findings, ZBG10 demonstrates exceptional anti-wear properties against zirconia balls in SBF solution, while the ZBG0 sample exhibits a significantly poorer wear rate.

The wear rate of a material is primarily influenced by its mechanical properties, such as hardness, density, elastic modulus, applied load, and Hertzian contact pressure, as well as the hardness of the mating material (Pandey *et al.*, 2023). Specifically, the wear rate is closely tied to the H/E (hardness/elastic modulus) ratio (Ehtemam-Haghighi *et al.*, 2016). The density and hardness of the composite samples were previously determined and documented in the Chapter 4. It was found that the density and mechanical properties of 3Y-TZP were enhanced with the addition of BG up to 10 wt%, but subsequently decreased with further BG additions up to 25 wt%. Furthermore, porosity was decreased with BG addition up to 10 wt%, after that, it increased up to 25 wt% Table 4.1 of Chapter 4. The incorporation of BG into 3Y-TZP up to 10 wt% can fill voids and compact the samples, thereby potentially enhancing wear resistance reported in Chapter 4. This compactness may explain the lower wear rate observed in the ZBG10 sample against the zirconia ball. Overall, the addition of BG to 3Y-TZP ceramics shows promise in improving wear resistance and reducing wear rate and volume up to 10 wt% of BG addition, making them more suitable for biomedical and other load-bearing applications.

8.2.4 Worn surface characterization

Fig. (8.4, 8.5 & 8.6) shows the HR-SEM image and EDS analysis of the worn surfaces of composite samples (ZBG0, ZBG5, ZBG10, ZBG15, and ZBG25) over two distinct magnifications (Fig. 8.4 & Fig. 8.5), respectively. Table 8.1 shows the wear scar width is lowest for the ZBG10 sample and highest for the ZBG0 sample. This data matches up with the HR-SEM image, as shown in Fig.8.4. This image indicates that wear scar width is the lowest in the ZBG10 sample and highest in the ZBG0 sample. The average COF value of the ZBG0 sample is maximum compared to all other four samples, as represented in Fig. 8.2(b).

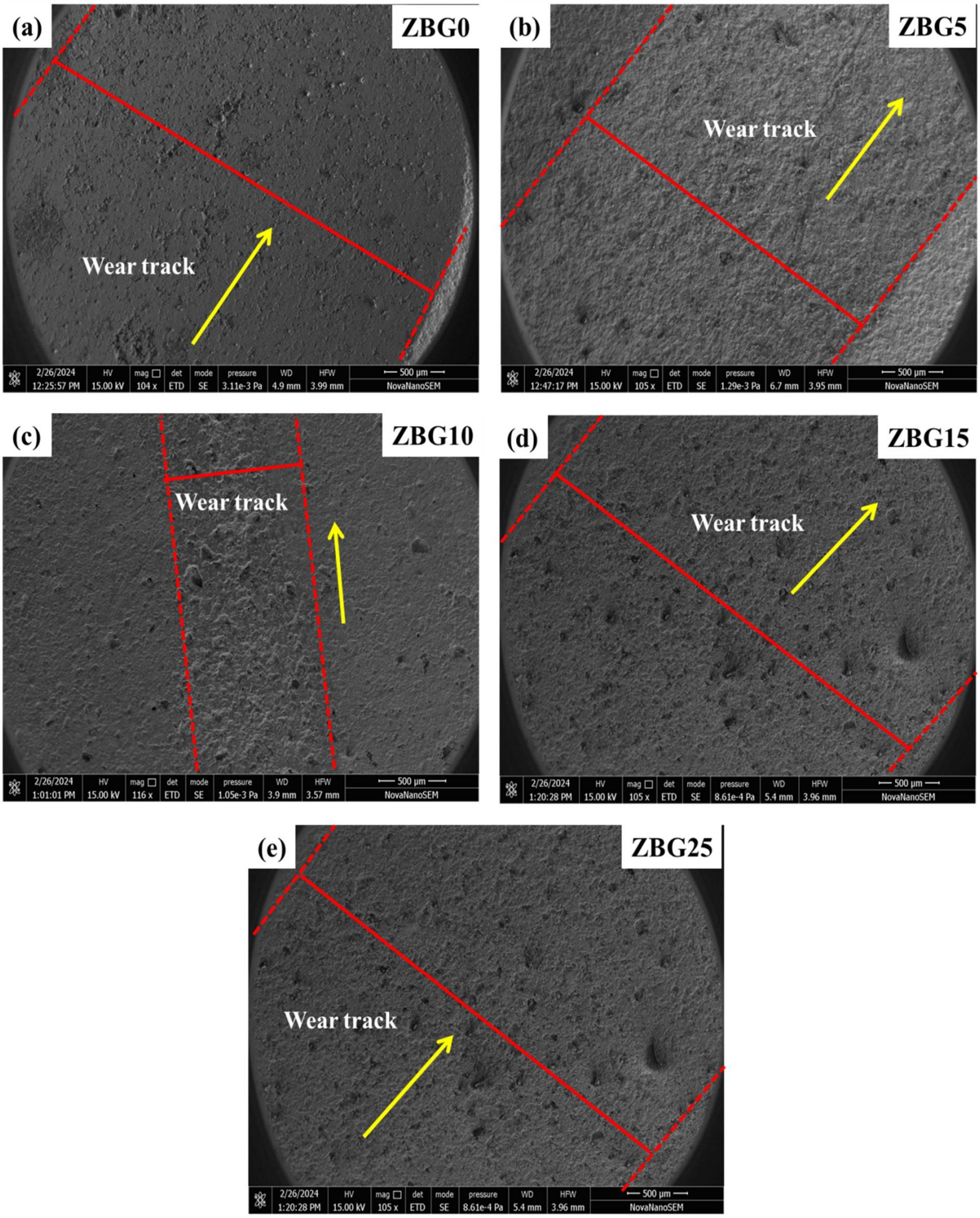

Fig. 8.4 HR-SEM images of the wear track (105X) magnification.

This COF variation conforms well with the HR-SEM image of the worn surface of ZBG0 (Fig. 8.4(a)) and ZBG10 (Fig. 8.4(b)) sample. The multiple scratches may lead to maximum friction, and low scratches lead to minimum friction on the worn surfaces. The multiple scratches are observed in HR-SEM images of the worn surfaces of the ZBG0 sample that support the COF data of the same.

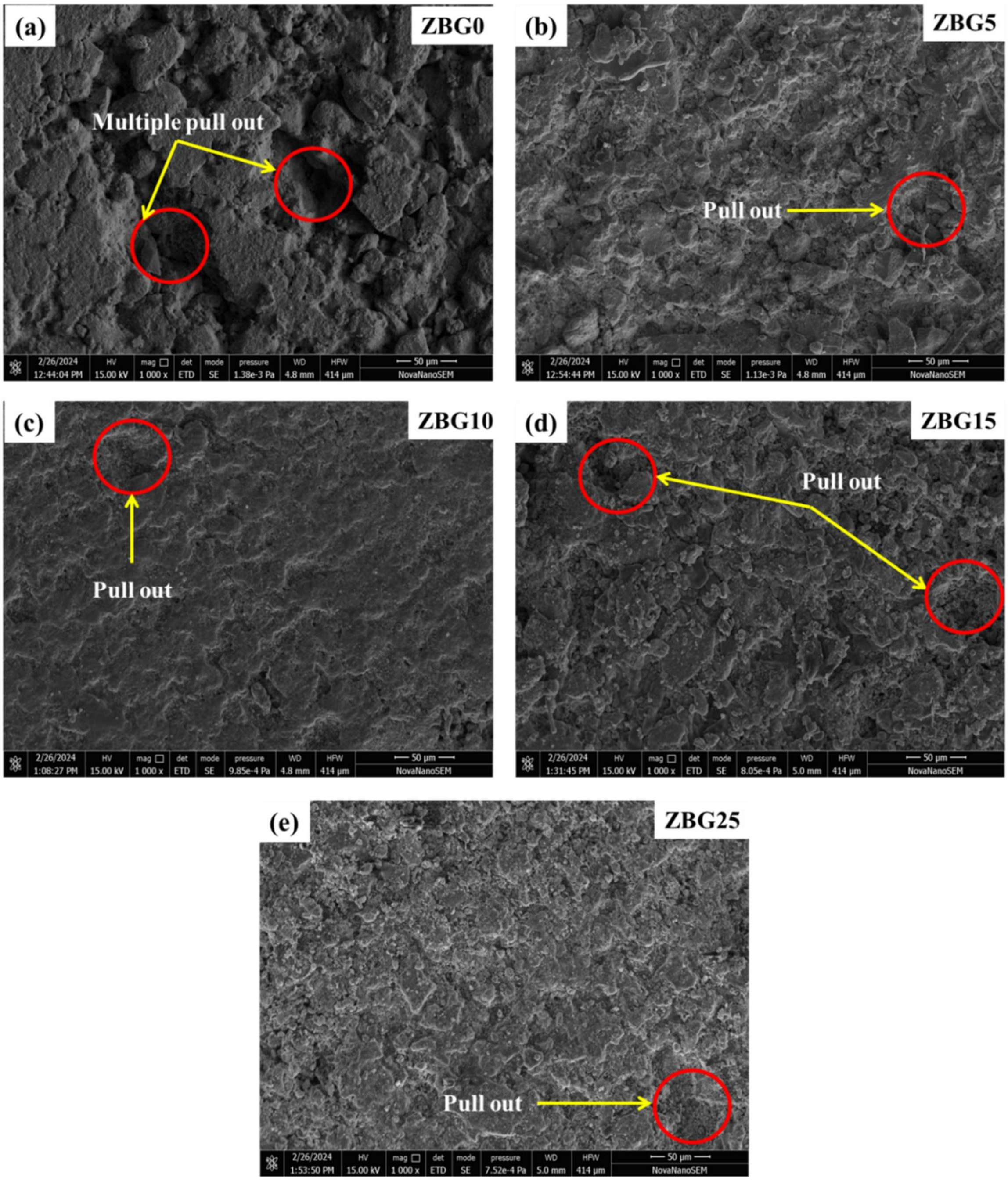

Fig. 8.5 HR-SEM images of the wear track (1000X magnification).

One potential explanation for the highest level of scratches is the premature degradation of the sample's surface layer, leading to direct contact between the zirconia ball and the sample surface. Likewise, the ZBG5 sample exhibits a lower average COF compared to the ZBG0 sample, and the lowest among all samples, as represented in Fig. 8.2(b).

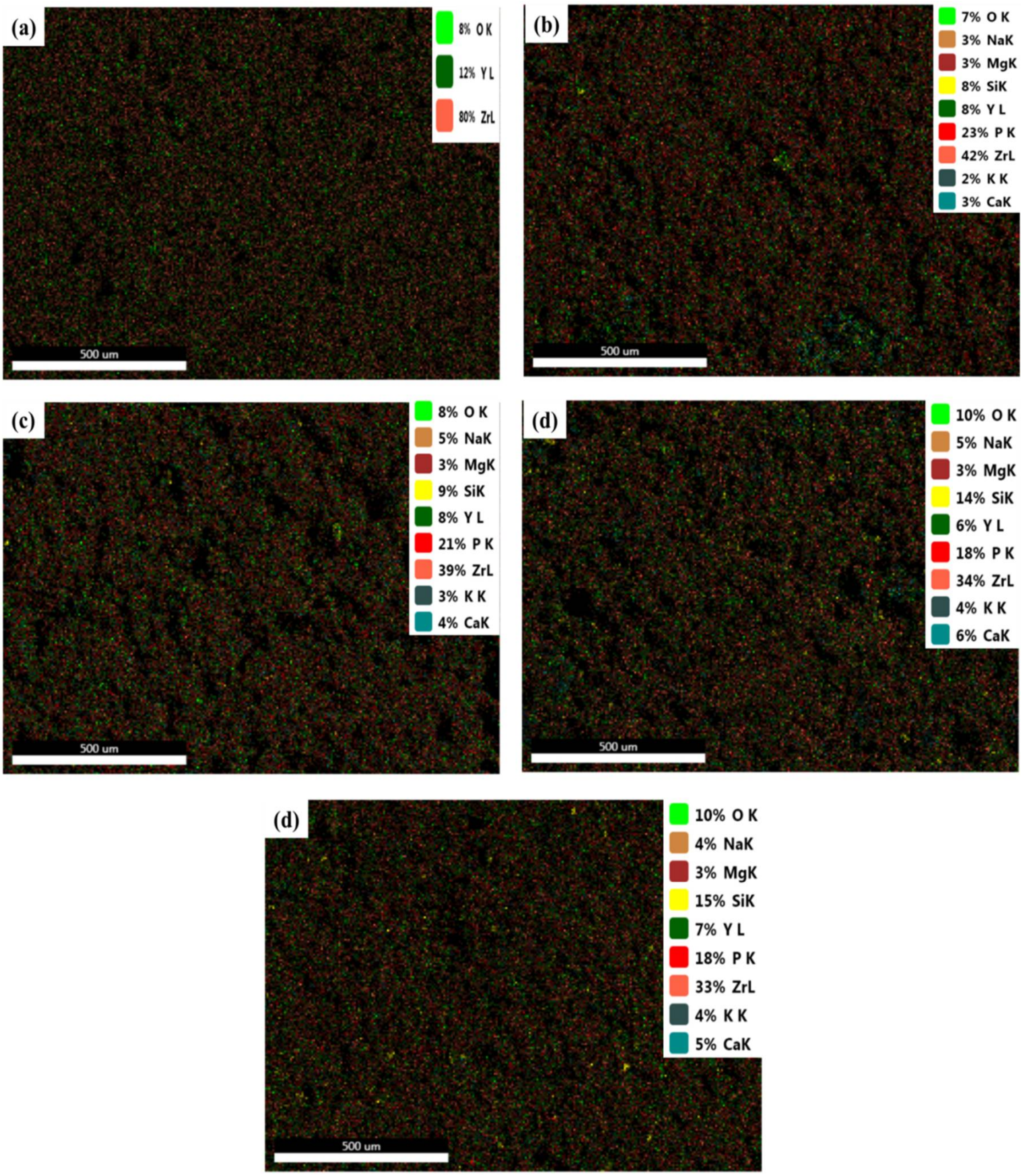

Fig. 8.6 EDS spectra of worn surfaces of all composite samples.

The reduction in COF may be due to the fewer scratches formed on the sample surfaces. This fact may be observed in SEM images of ZBGO, ZBG5, and ZBG10 samples, in which fewer scratches are formed as shown in Fig. 8.5(a, b, & c). Further, the average COF value of the ZBG15 and ZBG25 samples is increased as compared to the ZBG10 sample, shown in Fig. 8.2(b). Again more scratches are observed in the SEM images of ZBG15, and ZBG25 samples, as shown in Fig. 8.5(d, & e). Overall, HR-SEM pictures of worn surfaces reveal that both material pull-out and micro-cutting wear mechanisms are present in all samples, with pull-out being the major wear mechanism. The EDS mapping of all samples is shown in Fig. 8.6(a)-(e). The elements Zr, Y, Si, Ca, Na, Mg, K, P, and O are present on the worn surface of samples. Also, it is observed that all the elements are dispersed uniformly. Further, it is found that the wt% of the Zr element is decreased with increasing the BG concentration.

8.2.5 Surface profilometry analysis

Table 8.2 The details of surface roughness of worn surface after wear experiment.

Sample Code	Line roughness			Surface roughness	
	Ra (µm)	Rq (µm)	Rz (µm)	Sz (µm)	Sa (µm)
ZBG0	1.754	2.129	9.475	3.445	2.780
ZBG5	1.684	2.058	9.429	3.580	2.894
ZBG10	1.813	2.258	10.31	3.434	2.780
ZBG15	2.012	2.433	10.84	3.990	3.222
ZBG25	2.111	2.583	10.87	3.586	2.877

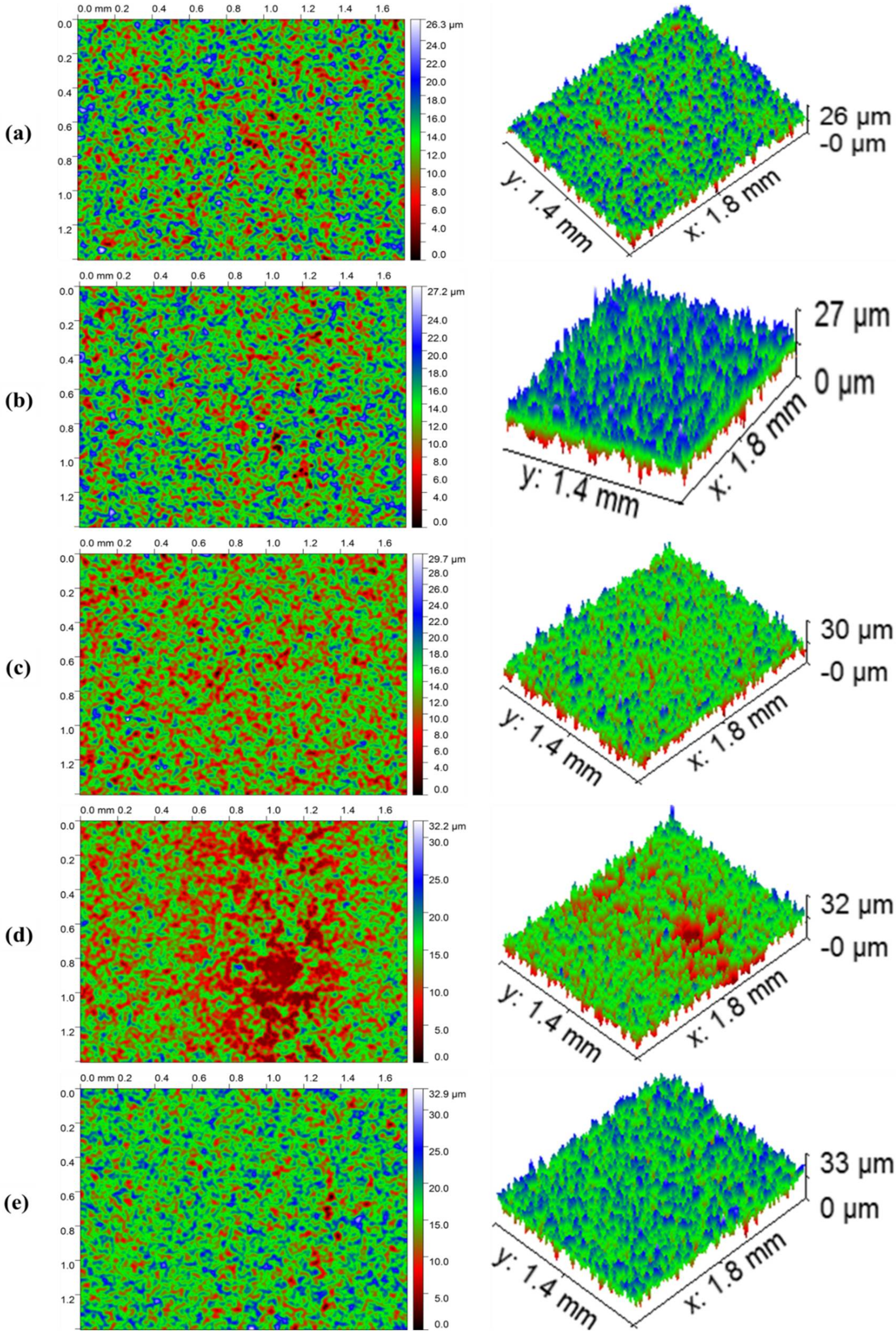

Fig. 8.7 Worn surface topography (Left side 2D and Right side corresponding 3D image) of the composite samples (a) ZBG0, (b) ZBG5, (c) ZBG10, (d) ZBG15, (e) ZBG25 at 20 N.

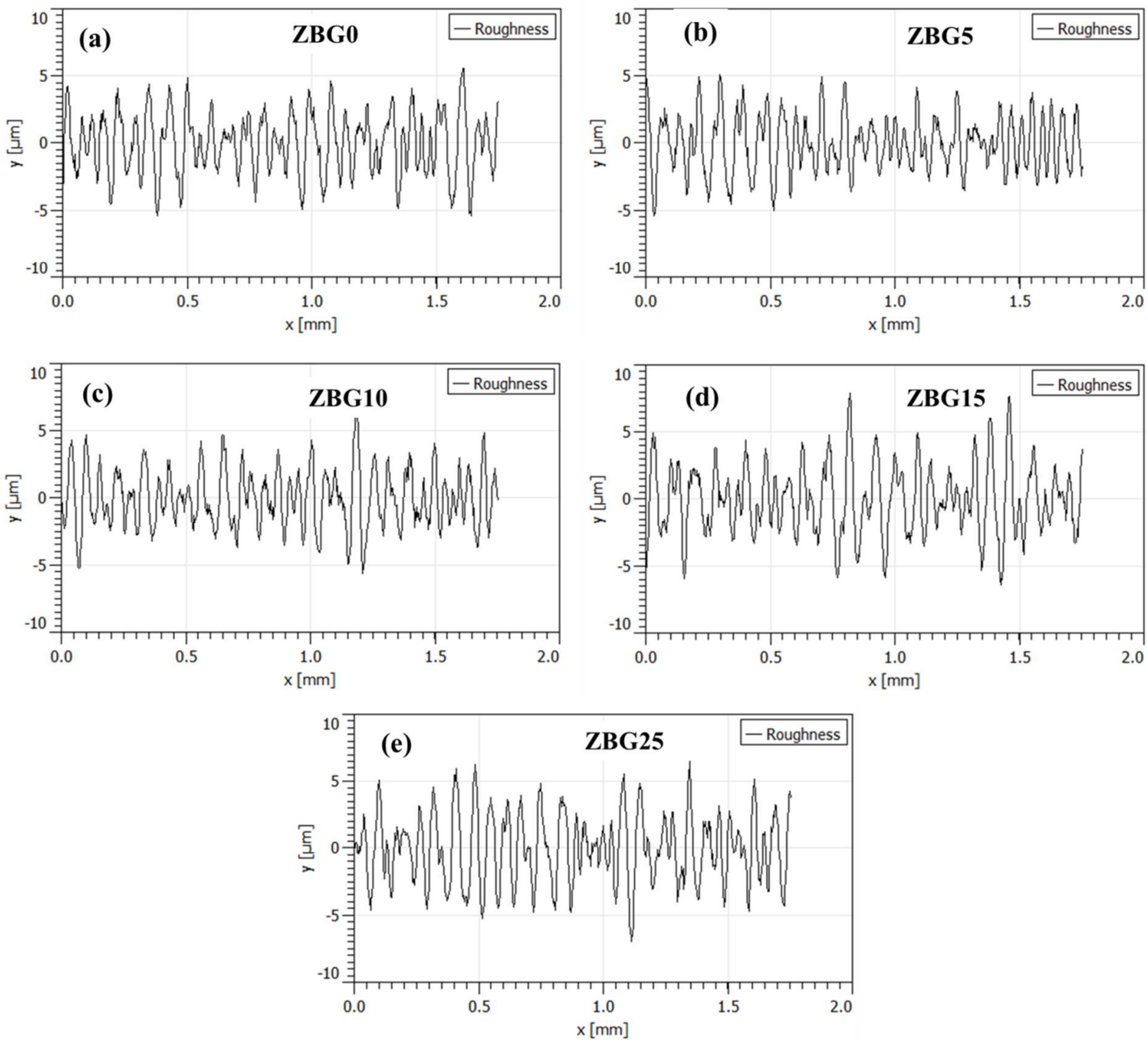

Fig. 8.8 Worn surface roughness pattern of 3Y-TZP/BG (0 to 25 wt%) composites.

The study of worn surfaces is conducted using an optical profilometer, with the roughness profile, as depicted in Fig. 8.7. The roughness profiles for composite samples are presented in two-dimensional (2D) on the left side and three-dimensional (3D) on the right side in Fig. 8.7. Gwyddion software is utilized to analyze the profile, with roughness parameters, as displayed in Table 8.2. Parameters such as Rz and Ra represent the maximum height and average roughness along a line, respectively. Conversely, Sa and Sz denote the average roughness and maximum height across the entire area. The line roughness parameters (Ra, Rq, and Rz values) are almost increased with increasing the BG contents (0 to 25 wt%).

Similarly, the surface roughness parameters (Sa and Sz) are also almost enhanced with enhancing BG contents (to 25 wt%) with a slight decrement in the ZBG25 sample. The surface roughness pattern of all composite samples obtained by optical profilometer is shown in Fig. 8.8. The surface quality of worn surfaces is destroyed by the porosity and cracks present on the surface of the sample. The porosity and hardness of the material are increased by increasing the BG content, as reported in the Chapter 4, which may be a strong reason for the poor surface finish associated with BG concentration (0 to 25 wt%). An additional reason may be that when BG is added to 3Y-TZP, the matrix becomes moist, and the grain becomes a larger, more asymmetrical shape, leading to enhanced surface roughness. As discussed in Chapter 4 that SR is enhanced as BG addition increases.

8.3 Summary

3Y-TZP-based BG bioceramic composites are prepared by powder metallurgy route. The effects of different content of BG (0 - 25 Wt%) on the COF, and wear rate of the of 3Y-TZP ceramics are studied. The wear rate and COF are significantly dependent on the bioactive glass concentration inclusions in SBF to the ZrO_2 counterpart. The wear rate and COF are decreased with BG content up to 10 wt%. Afterward, it is increased up to the BG 25 wt%. The wear resistance of the ZBG10 sample is excellent owing to its good microstructure and mechanical properties. It has also the lowest COF than other samples. All composite samples undergo micro-cutting during the wear test. Good hardness and good bond strength between grains only cause slightly less wear scar in ZBG10 than in the other samples. Line and surface roughness are increased with increasing the BG content in 3Y-TZP ceramic. Table 8.3 correlates the findings of this experiment with those of earlier reported research on the tribological response of characteristics of the current material.

Table 8.3 Correlates the findings of the current study with those of earlier reported research on the tribological response of the current material.

S. No.	Materials	Wear test Method /Instrument	Wear rate and COF response
1	Ceria stabilized zirconia (CSZ) (Pandey *et al.*, 2014)	Fretting wear test at different loads was carried out using balls on flat geometry	Hydrothermal treatment improved the hardness and wear resistance
2	Zirconia reinforced by 10 vol% of HAp and by 10 vol% of β-TCP (Pandey et al., 2014) (Buciumeanu *et al.*, 2018)	Wear tests were carried out in Phosphate Buffered Saline (PBS) solution at 37 ± 2 ºC using a ball-on-plate configuration	The tribological performance was not affected by the addition of bioactive materials. No change in wear rates and COF
3	3Y-TZP Ceramic (Buciumeanu *et al.*, 2018)	The reciprocating frictional experiments, against the Si_3N_4 ball under dry and distilled water-lubricated conditions	The feasibility of preparing micro textures onto the surface, which enhanced the wettability, and tribological behaviors of 3Y-TZP ceramics
4	Mullite/3Y-TZP ceramics (Huang *et al.*, 2019)	Multifunctional friction and wear tester	Mullite uniformly distributed into ZrO_2, reduced porosity leading to low COF
5	Silica infiltrated zirconia (Alves *et al.*, 2022)	-	Silica infiltration resulted in lower wear of the zirconia
6	Glass-ceramics reinforced by 3Y-TZP (Pandey *et al.*, 2014)	The wear tests were carried out using a ball-on-plate configuration	Moderate wear response
7	3Y-TZP/Ta (20 vol%) (Santos *et al.*, 2016)	Pin (UHMWPE)-on-flat wear test under dry conditions	Showed high resistance to low-temperature degradation and good tribological properties

8	ZrO_2-doped borosilicate glasses (Smirnov *et al.*, 2018)	pin-on-disk tribometer	The addition of ZrO_2, to borosilicate glass improved its mechanical properties and also increased the wear resistance.
9	Zirconia–MWCNTs composites (Jain *et al.*, 2023)	An automatic tribometer in reciprocating dry sliding conditions, using ball-on-disc geometry	At low loads, the addition of MWCNTs increased the COF and clearly decreased the wear rate, under high loads, the composites develop chipping and brittle fracture as MWCNT content increased
10	Present work 3Y-TZP/BG Composite	Biotribometer, For bio implant	Improved wear resistance and COF up to 10 wt% of BG addition into 3Y-TZP ceramics